Original Article

Delayed contrast-enhanced magnetic resonance imaging enables detection of pulmonary artery lesions in Takayasu's arteritis

Xiaojuan Guo[1], Min Liu[2], Mingxi Liu[1], Zhanhong Ma[1], Juanni Gong[3], Yuanhua Yang[3], Wei Gao[4], Jiaoyan Wu[5], Qi Yang[1#], Min-Fu Yang[5#]

[1]Department of Radiology, Beijing Chaoyang Hospital, Capital Medical University, Beijing, China; [2]Department of Radiology, China-Japan Friendship Hospital, Beijing, China; [3]Department of Pulmonary and Critical Care Medicine, Beijing Chaoyang Hospital, Capital Medical University, Beijing, China; [4]Department of Ultrasound, Beijing Chaoyang Hospital, Capital Medical University, Beijing, China; [5]Department of Nuclear Medicine, Beijing Chaoyang Hospital, Capital Medical University, Beijing, China

Contributions: (I) Conception and design: MF Yang; (II) Administrative support: Q Yang; (III) Provision of study materials or patients: Y Yang, J Gong; (IV) Collection and assembly of data: Mingxi Liu, Z Ma, W Gao, J Wu; (V) Data analysis and interpretation: X Guo, Min Liu; (VI) Manuscript writing: All authors; (VII) Final approval of manuscript: All authors.

[#]These authors contributed equally to this work and should be considered as co-corresponding authors.

Correspondence to: Qi Yang. Department of Radiology, Beijing Chaoyang Hospital, Capital Medical University, 8th Gong Ti Nan Road, Chao Yang District, Beijing 100020, China. Email: yangyangqiqi@gmail.com; Min-Fu Yang. Department of Nuclear Medicine, Beijing Chaoyang Hospital, Capital Medical University, 8th Gong Ti Nan Road, Chao Yang District, Beijing 100020, China. Email: minfuyang@126.com.

Background: Delayed contrast-enhanced magnetic resonance imaging (DE-MRI) is a useful technique to identify arterial wall inflammation. The aim of this study was to explore the value of DE-MRI in the evaluation of pulmonary artery (PA) lesions in Takayasu's arteritis (TAK) compared with ^{18}F-fuorodeoxyglucose positron emission tomography/computed tomography (^{18}F-FDG PET/CT).

Methods: Patients with TAK were recruited for this prospective, observational study. Imaging and clinical assessments were performed concurrently. Only thoracic arteries were evaluated, and they were divided into 18 segments per person. All arterial lesions were evaluated using both PET/CT and DE-MRI. Correlations between both methods were assessed in the PA and thoracic aorta. A receiver operating characteristic (ROC) curve was used to analyze the value of imaging features in detecting disease activity based on National Institutes of Health (NIH) criteria.

Results: A total of 24 patients contributed 432 arterial segments. Using PET/CT, correlations between arterial wall DE, thickening, and edema in the PA were 84.52%, 67.92%, and 58.33%, respectively, with Cohen's kappa =0.69, 0.30, and 0.13, respectively; for the thoracic aorta, the values were 86.38%, 80.00%, and 75.92%, respectively, with Cohen's kappa =0.71, 0.52, and 0.37, respectively. There was a significant difference in the incidence of wall DE between the PA and thoracic aorta in patients with clinically active TAK (χ^2=6.85, P=0.009). DE-MRI presented a higher area under the curve [area under the curve (AUC); 0.729, P=0.047] than wall thickening and edema in the detection of TAK activity. The wall DE combined with erythrocyte sedimentation rate (ESR) showed improved efficiency (AUC: 0.858, P=0.003).

Conclusions: DE-MRI displays appreciable correlations with PET/CT findings and allows for the detection of PA inflammation in patients with TAK; it shows higher values in the thoracic aorta than in the PA. The combination of wall DE and ESR can improve the efficiency of assessing disease status.

Keywords: Delayed contrast-enhanced magnetic resonance imaging (DE-MRI); fluorodeoxyglucose positron emission tomography/computed tomography (FDG PET/CT); Takayasu's arteritis (TAK); pulmonary artery (PA)

Submitted Feb 20, 2022. Accepted for publication Oct 24, 2022. Published online Nov 24, 2022.
doi: 10.21037/qims-22-130
View this article at: https://dx.doi.org/10.21037/qims-22-130

Introduction

Takayasu's arteritis (TAK) is a rare, chronic large vessel vasculitis (LVV), which predominantly affects the aorta and its major branches. It is characterized by granulomatous inflammation and thickening of the arterial wall, with subsequent remodeling resulting in stenosis, occlusions, or ectasia/aneurysms (1,2). Pulmonary artery (PA) involvement in TAK is uncommon, with the prevalence of PA involvement (PAI) ranging from 6.9% to 36.7% in all patients with TAK (3). Patients with PAI present with different clinical features than other TAK patients as well as a higher mortality rate (23%) than that of TAK patients overall (4). Accurate assessment of PA is especially important for timely and proper treatment to improve prognosis. Unfortunately, vascular progression is difficult to predict, and disease activity assessment remains an unresolved conundrum for TAK patients with PAI (5).

Magnetic resonance imaging (MRI) is a useful noninvasive imaging method for identifying arterial wall abnormalities, and it is considered reflective of disease activity in patients with TAK. MRI studies of TAK are mainly associated with circulatory system vessel lesions, such as those of the aorta and its branches. Research has shown that patients with unequivocal clinically active TAK have a high frequency of vessel wall edema (6). The vessel locations of LVV with wall edema and thickening captured on MRI show an association with ^{18}F-fluorodeoxyglucose (^{18}F-FDG) positron emission tomography/computed tomography (PET/CT) scan activity, which makes these locations a more useful imaging feature (7). Delayed contrast-enhanced MRI (DE-MRI) has also been shown to be a useful technique to identify inflammation in the arterial wall and can, therefore, identify TAK-related disease activity (8). One study found that vessel contrast-enhancement resolved in 42% patients with LVV using biological therapies (9). However, the PA wall is thinner compared with that of the aorta and its branches, and it requires a higher resolution imaging method. Studies that focus on PA lesions associated with TAK are limited.

According to our clinical experience and previous studies, patients with clinically suspected PAI rarely display PA wall edema and thickening (10). Additionally, we could not retrieve any articles about the evaluation of PA wall edema and wall thickening using MRI in TAK patients. However, PA lesions presenting as wall DE have been detected by MRI using a three-dimensional (3D) inversion recovery Turbo FLASH sequence (10), which is very helpful in identifying patients with suspected active TAK and PAI (11).

Several studies have shown that PET/CT is a sensitive and specific imaging tool for evaluating LVV (12-16), and ^{18}F-FDG uptake is associated with clinical disease activity and a biomarker of inflammation to monitor treatment response (17-19). Thus, PET/CT is currently considered the most valuable imaging method for identifying TAK disease status. We have also investigated the value of PET/CT in displaying PA activity in TAK and found that PET/CT, with higher specificity [PET/CT (91.7%) *vs.* wall thickness (37.5%), P=0.001] and accuracy [PET/CT (84.2%) *vs.* wall thickness (57.9%), P=0.022], was superior to wall thickness on MRI or CT angiography (20). However, PET/CT has lower resolution compared with DE-MRI, which limits the ability to detect PA lesions. In addition, due to radiation exposure, it is not suitable for the follow-up of young patients, and as it is more expensive than DE-MRI, it is less widely available.

DE-MRI is useful in detecting the extent of vessel wall inflammation in patients with TAK (6,21). Whether or not arterial wall active inflammation in TAK using DE with gadolinium-based contrast agent is associated with ^{18}F-FDG uptake on PET/CT requires assessment. Thus, we hypothesized that DE-MRI will be able to detect active PA lesions when compared with PET/CT and will be valuable in assessing the clinical activity of TAK.

The primary objectives of this study were as follows: (I) to explore the utility of DE-MRI as a method to detect active PA lesions in TAK when compared with PET/CT; (II) to analyze the difference of wall DE between the PA and thoracic aorta in patients with TAK; and (III) to assess the value of wall DE in assessing clinical activity in patients with TAK. We present the following article in accordance with the STARD reporting checklist (available at https://qims.amegroups.com/article/view/10.21037/qims-22-130/rc).

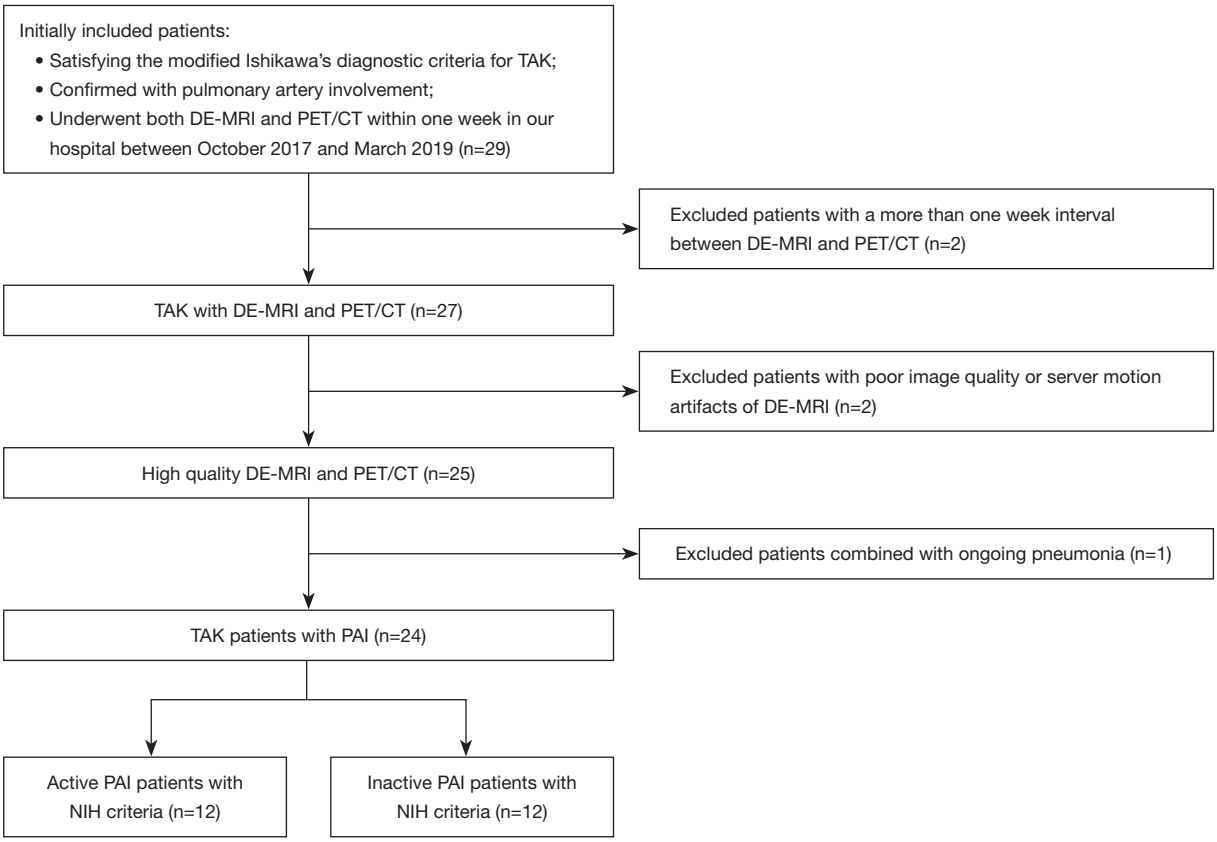

Figure 1 Flowchart outlining the population selection of the final study. TAK, Takayasu's arteritis; DE-MRI, delayed contrast-enhanced magnetic resonance imaging; PET/CT, positron emission tomography/computed tomography; PAI, pulmonary artery involvement; NIH, National Institutes of Health.

Methods

Patient selection and evaluation

From October 2017 to March 2019, 29 patients who attended Beijing Chaoyang Hospital, Capital Medical University for respiratory symptoms satisfying the modified Ishikawa's diagnostic criteria for TAK (20) underwent both DE-MRI and PET/CT within 1 week and were consecutively enrolled in this study. The sample size of this study was estimated using diagnostic test methods based on our previous research (21). The final sample included 24 patients, who were classified as having either clinically active or inactive TAK according to the validated National Institutes of Health (NIH) criteria (22) as assessed by clinicians without knowledge of the imaging findings (*Figure 1*). The laboratory results, including erythrocyte sedimentation rate (ESR) and C-reactive protein (CRP), were measured within 1 week of imaging.

The patients of this imaging subgroup analysis were included in a prospective study on TAK, which was approved by the Ethics Committee of Beijing Chaoyang Hospital (No. 2017-K-127), and all participants were aware of, and agreed to participate in, this study. The study was conducted in accordance with the Declaration of Helsinki (as revised in 2013). Informed consent was provided by all individual participants included in the study.

MRI acquisition

All patients underwent MRI on a 3.0-T scanner (Prisma; Siemens Healthcare, Erlangen, Germany) with a body-flex receiver coil. After scout imaging, Short T1 Inversion Recovery (STIR) T2-images were first acquired to detect mural edema, using a T2_ Turbo Spin Echo _ Fat saturation sequence with the following parameters: repetition time/echo time (TR/TE) 1,890/70 ms, thickness 5 mm, field of

view (FOV) 300 mm × 340 mm, and voxel size 1.3 mm × 1.3 mm × 5 mm. Then, magnetic resonance angiography (MRA) was performed with Angio3D sequence (TR/TE 2.99/1.06 ms, a flip angle of 23°, FOV 500 mm × 400 mm, thickness 1.1 mm, and voxel size 1.2 mm × 1.2 mm × 1.1 mm) at 5–8 s after injection of gadopentetate dimeglumine (Magnevist; Schering, Berlin, Germany). Gadopentetate dimeglumine was injected at 0.4 mmol/kg body weight at a rate of 3 mL/s followed by a 20–30 mL normal saline flush from a separate syringe at a rate of 2 mL/s.

DE-MRI was obtained at 10–15 min after injection of gadopentetate dimeglumine, using a coronial free-breathing 3D inversion recovery Turbo FLASH sequence. A crossed-pair navigator pulse was used for respiratory gating. Using a multiorientation image, the navigator pulse was located at a suitable site, whereby the right lower lobar artery was the least affected by artifacts. This protocol was applied to cover all large thoracic vessels (ascending aorta, aortic arch and its branches, thoracic descending aorta, main PA, and left/right PA and its branches). The typical imaging parameters were as follows: TR/TE 740/1.18 ms, flip angle 10°, data window duration 117 ms, FOV 340 mm × 400 mm, matrix 256×256, slices per slab 80, 1 slab, and voxel size 1.8 mm × 1.8 mm × 3.0 mm. The inversion time was individually optimized in each patient, and the inversion time was the same as the maximal suppression of the myocardium signal. The acceptable window of navigation was 2.5 mm, and respiratory motion adaptation was implemented.

MRI analysis

Two radiologists (MXL and XJG) with more than 5 years of imaging experience in cardiovascular disease, who were blinded to the clinical information and the PET/CT results, reviewed the images, and discrepancies were resolved by consensus. For segmental analysis, PA was divided into 10 segments, including 3 main segments (PA trunk and bilateral Pas) and 7 proximal branches (5 lobar arteries, right interlobar artery, and left lingual artery). In addition, 3 segments of the thoracic aorta (ascending artery, aortic arch, and descending artery) and 5 of its branches (brachiocephalic trunk, bilateral carotids, and bilateral subclavian arteries) were assessed. The luminal changes on MRA were classified into normal, stenosis/occlusion, and aneurismal dilatation. A positive DE was defined as a T1 signal intensity in the arterial wall that was higher than that of the myocardium signal at the same slice, and arterial wall edema was defined as a T2 signal intensity in the arterial wall that was higher than that of the chest wall muscle (23). The per-patient positive rate was counted based on the segments of positive MRI features divided by 18 total segments for each patient.

All 240 PA segments were included in wall DE analysis. The other MRI features (wall thickening, mural edema, and lumen) were included in the per-segment analysis in detail as shown in *Figure 2A*. Of the 192 thoracic aortic segments and branches, the included arterial numbers on MRI for per-segment analysis are shown in *Figure 2B*.

^{18}F-FDG PET/CT acquisition

To reduce the influence of myocardial ^{18}F-FDG uptake on the adjacent vessels, patients were instructed to fast for 15–18 h (mean 16.5±1.1 h), and unfractionated heparin (50 IU/kg of body weight) was intravenously administered. Then, the blood glucose level was measured. If the patients had a blood glucose level of <126 mg/dL, ^{18}F-FDG was intravenously administered (3.7 MBq/kg). PET/CT scans were performed on a GE Discovery STE device (GE Healthcare, Chicago, IL, USA) using a standard protocol. To increase the vascular-to-blood ratio, whole-body ^{18}F-FDG PET/CT scans were obtained 120–150 min after ^{18}F-FDG administration (24,25). The CT parameters were as follows: 140 kV, 120 mA, pitch 1.375, and section width of 5 mm. The PET acquisition parameters were as follows: 2.5 min/bed from the skull base to the middle of the thighs, 3D mode, a matrix size of 128×128, and a 70 cm FOV. The PET images were reconstructed using a 3D ordered-subset expectation maximization algorithm with 2 iterations and 14 subsets, and a slice thickness of 3.27 mm. Integrated PET and CT images were obtained automatically on AW VolumeShare2 (GE Healthcare).

^{18}F-FDG PET/CT analysis

Images were independently reviewed by 2 nuclear physicians (JW and MFY) with more than 3 years of imaging experience in cardiovascular disease, who were blinded to patients' clinical information and the MRI results, and discrepancies were resolved by consensus. The same PA and thoracic segments as for the MRI were evaluated semiquantitatively by measuring the maximum standardized uptake value (SUV_{max}). A two-dimensional (2D) region of interest (ROI) was manually drawn around the vascular wall in contiguous axial slices, and another ROI was drawn in the right lobe of the liver. The target-to-background ratio was calculated as the SUV_{max} of the vascular wall divided by the SUV_{max} of the

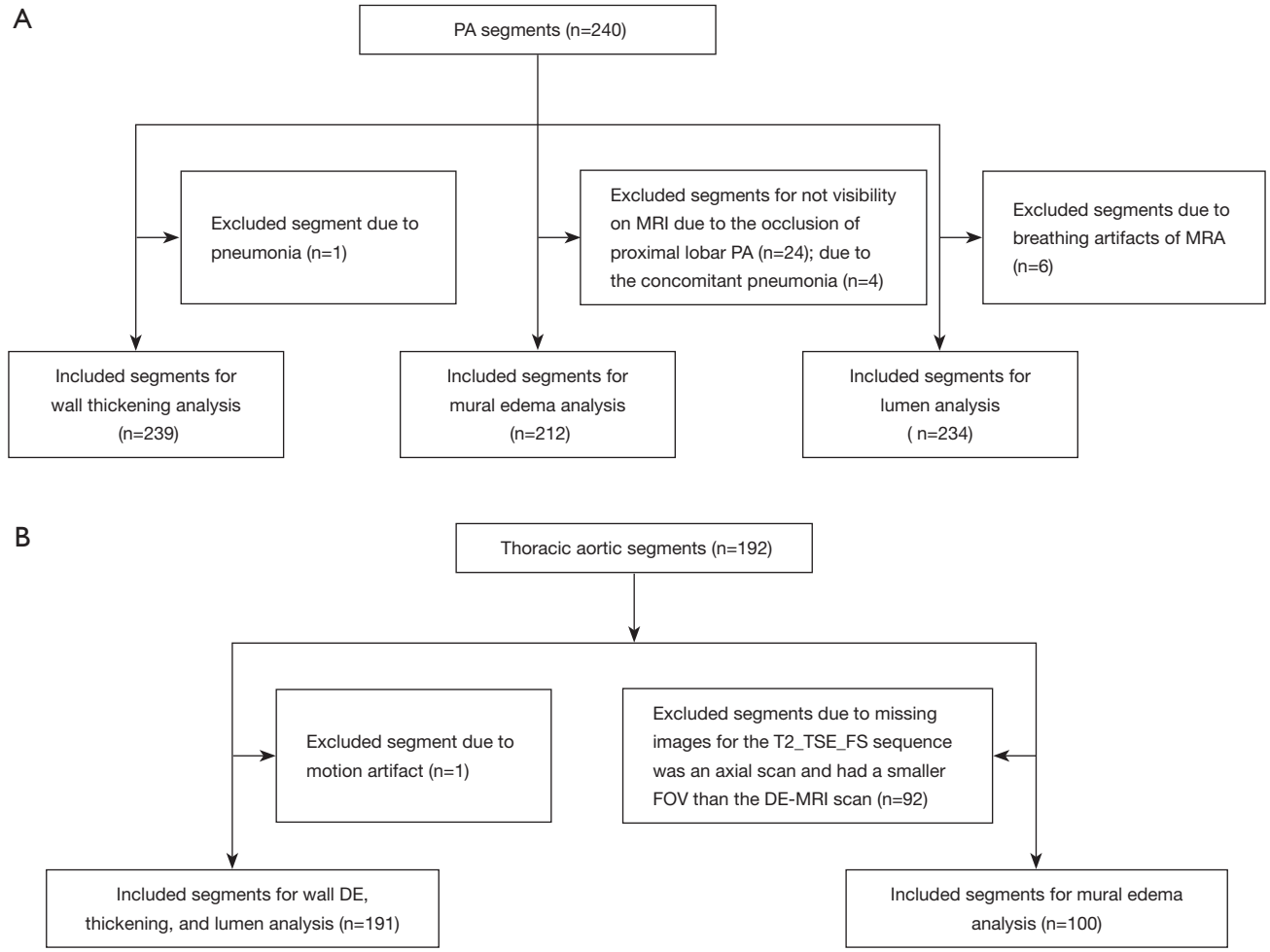

Figure 2 Flowchart outlining the included segments for PA analysis (A) and thoracic aortic artery analysis (B). PA, pulmonary artery; MRA, magnetic resonance angiography; MRI, magnetic resonance imaging; DE, delayed contrast-enhanced; TSE, turbo spin echo; FS, fat saturation; FOV, field of view.

liver, and a vascular segment with the target-to-background ratio ≥1 was considered active (21).

Statistical analysis

Quantitative data were expressed as mean ± standard deviation or median with a range depending on the distribution of data. Values for qualitative variables were expressed as percentages. Consistency evaluation was conducted by percentage overall agreement with Cohen's kappa test. An independent-sample *t*-test or Mann-Whitney U test was used as appropriate for comparison of quantitative variables, and the associations of qualitative data were evaluated using a chi-square test or Wilcoxon test for subgroup analysis. Spearman's rho correlation analysis was performed to detect the relationship between MRI features and acute phase serum reactants. Receiver operating characteristic (ROC) curve analysis was used to evaluate the diagnostic accuracy of each imaging feature. All statistical analyses were performed using the software SPSS 20.0 (IBM Corp., Armonk, NY, USA). A two-tailed P value <0.05 was considered statistically significant.

Results

Study population

The demographic and clinical features of the enrolled patients are shown in *Table 1*. A total of 12 patients were

Table 1 Characteristics of enrolled patients (n=24)

Variables	Results
Female, n (%)	18 (75.00)
Age (years)*	37±12
Disease duration (months)#	10 (1–360)
BMI (kg/m^2)*	22.64±3.55
Active disease at enrollment (NIH criteria), n (%)	12 (50.00)
Clinical manifestation, n (%)	
Pulse deficits	2 (8.33)
Chest pain	13 (54.17)
Dyspnea	10 (41.67)
Fever	11 (45.83)
Cough	15 (62.50)
Expectoration	11 (45.83)
Hemoptysis	7 (29.17)
Treatment at enrollment, n (%)	
Steroid therapy	6 (25.00)
Steroid and cyclophosphamide therapy	5 (20.83)
Antiplatelet drugs	11 (45.83)
Antihypertensive drugs	4 (16.67)
Blood glucose at PET scan (mg/dL)*	5.34±0.71
ESR (mm/h)#	18 (2–84)
CRP (mg/L)#	0.95 (0.16–11.10)

*, data presented as mean ± standard deviation; #, data represented as median (minimum and maximum values). BMI, body mass index; NIH, National Institutes of Health; PET, positron emission tomography; ESR, erythrocyte sedimentation rate; CRP, C-reactive protein.

considered to have clinically active TAK at the time of enrolment. ESR [median (range), 41 (2–84) mm/h] and CRP [median (range), 1.84 (0.40–11.10) mg/L] in patients with active TAK were higher compared than those with inactive TAK [ESR, median (range), 9.5 (2–61) mm/h; CRP, median (range), 0.445 (0.16–3.00) mg/L]. There were significant differences between the 2 groups in ESR (Z =–2.32, P=0.02) and CRP (Z =–2.25, P=0.024). The interval between clinical diagnosis and imaging examination was no more than 1 week, during which time the patient received the appropriate treatment. A total of 11 patients received steroid and/or immunosuppressive therapy.

Association of DE-MRI and acute phase serum reactants

Notably, 66.67% (8/12) of patients in clinical remission had imaging activity on DE-MRI (*Figure 3*). We used the per-patient positive rate to quantitatively analyze the relationship between MRI features and acute phase serum reactants. Additionally, there was no statistical association between the positive rate of segmental wall DE and the ESR (rho =0.025, P=0.93) or the CRP level (rho =0.226, P=0.48) for 12 of the patients with clinically active TAK.

Association of arterial wall DE and PET/CT findings

As shown in *Table 2*, a total of 240 (100%) PA segments and 191 (99.48%) thoracic aorta segments were assessed for consistency analysis of segmental wall DE on MRI and positive PET/CT (*Figures 4*,*5*), and the percentage of agreement of 75.92% with Cohen's kappa =0.37 (P<0.001) in the thoracic aorta was higher than that in the PA (*Figures 6*,*7*).

Association of arterial wall DE and other MRI features

As shown in *Tables 3*,*4*, 239 (99.58%) PA segments and 191 (99.48%) thoracic aorta segments were included in the consistency analysis of wall DE and thickening, and 212 (88.33%) PA segments and 100 (52.08%) thoracic aorta segments were included in the consistency analysis between wall DE and edema (*Figures 6*,*7*). The result indicated that there was considerable agreement between wall DE and thickening and edema, but the agreement between wall DE and thickening was higher than that between wall DE and edema. Moreover, the consistency of MRI features in the thoracic aorta (the percentage of overall agreement between wall DE and thickening and edema =86.38% and 80.00%, respectively, with Cohen's kappa =0.71 and 0.52, respectively) was higher than that for PA (the percent overall agreement between wall DE and thickening and edema =84.52% and 67.92%, respectively, with Cohen's kappa =0.69 and 0.30, respectively). Wall DE showed no consistency with lumen abnormality in 234 (97.50%) PA segments and 191 (99.48%) thoracic aorta segments.

To detect differences in MRI features between the PA and thoracic aorta, a comparison was made between patients with active and inactive TAK, as outlined in *Table 5*. The incidence of wall DE in the PA was higher than that in the thoracic aorta in patients with both active (57.50% and 39.58%, respectively; P=0.009) and inactive TAK (37.50%

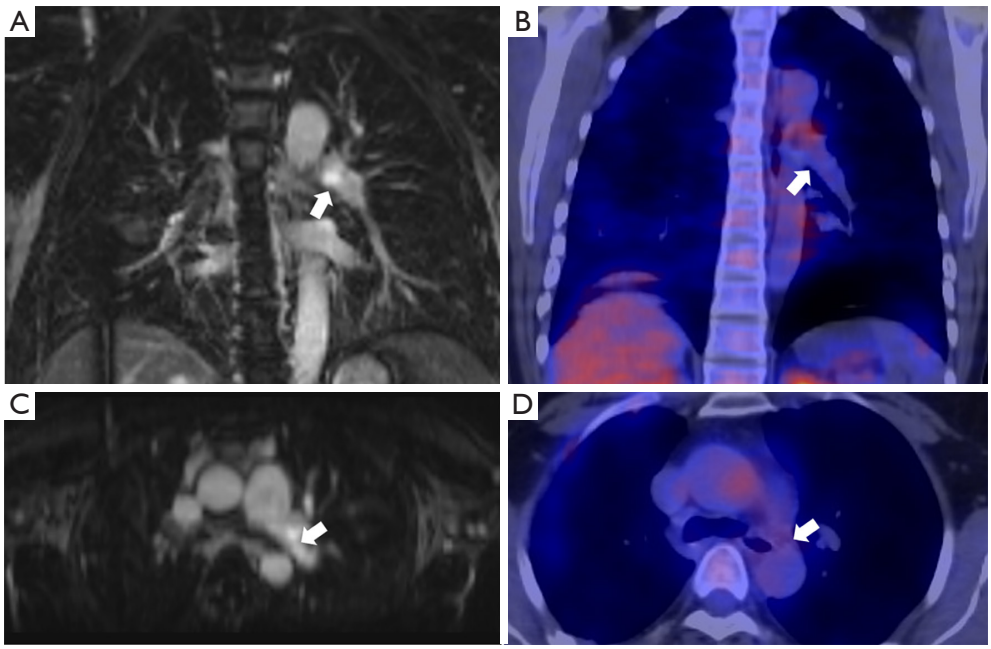

Figure 3 A 42-year-old female patient, who received steroid and cyclophosphamide therapy with active arteritis for 37 months and was in a clinically inactive phase. DE-MRI (A,C) shows arterial wall delayed enhancement in the left lower lobar artery (white arrows) in coronal and axial view. ^{18}F-FDG PET/CT images (B,D) show no uptake by the left lower lobar artery (SUV_{max} 2.8, liver SUV_{max} 2.9) (white arrows) in the same view. DE-MRI, delayed contrast-enhanced magnetic resonance imaging; FDG PET/CT, fluorodeoxyglucose positron emission tomography/computed tomography; SUV_{max}, maximum standardized uptake value.

Table 2 Per-segment comparison between arterial wall DE and PET/CT findings

Imaging features	PA		Thoracic aorta	
	DE-MRI+	DE-MRI–	DE-MRI+	DE-MRI–
^{18}F-FDG PET/CT+	20	6	23	5
^{18}F-FDG PET/CT–	94	120	41	122

PA (PET/CT& DE-MRI): Cohen's kappa =0.13 (P<0.001), percent agreement =58.33%. Thoracic aorta (PET/CT& DE-MRI): Cohen's kappa =0.37 (P<0.001), percent agreement =75.92%. DE, delayed contrast-enhancement; PET/CT, positron emission tomography/computed tomography; PA, pulmonary artery; DE-MRI, delayed contrast-enhanced magnetic resonance imaging; DE-MRI+/–, positive/negative delayed enhancement category in comparison to the myocardium signal; ^{18}F-FDG, ^{18}F-fluorodeoxyglucose; PET/CT+/–, focal positive/negative uptake in the arterial wall defined as a ratio of vascular uptake and liver uptake ≥1 or <1.

and 27.08%, respectively; P=0.105). However, the incidence of wall edema in the PA was lower than that in the thoracic aorta for both patients with active (19.23% and 29.17%, respectively; P=0.172) and inactive TAK (7.41% and 20.75%, respectively; P=0.004). Considering the incidence of wall thickening, there was no significant difference between PA and thoracic aorta in this study; however, lumen abnormality was more likely to occur in the PA compared with the thoracic aorta (93 *vs.* 3, P<0.001).

ROC analysis of disease activity based on MRI features and PET/CT findings

Following the NIH criteria, 12 patients were in the active phase. The ROC analysis using the per-patient positive rate of MRI features and the corresponding combined indicators in assessing disease activity are shown in *Figure 8*. The diagnostic performance of DE-MRI and PET/CT for the detection of TAK activity can be found in *Table 6*. The positive rate of wall DE showed the highest performance [area under the curve (AUC): 0.729, cut off value: 34.00%] for the detection of patients with active TAK among other MRI features [AUC of wall thickness: 0.67, 95% confidence interval (CI): 0.45–0.90, P=0.149; AUC of wall edema: 0.66, 95% CI: 0.43–0.88, P=0.194], but it was inferior to that of PET/CT. When the positive rate of wall DE was combined

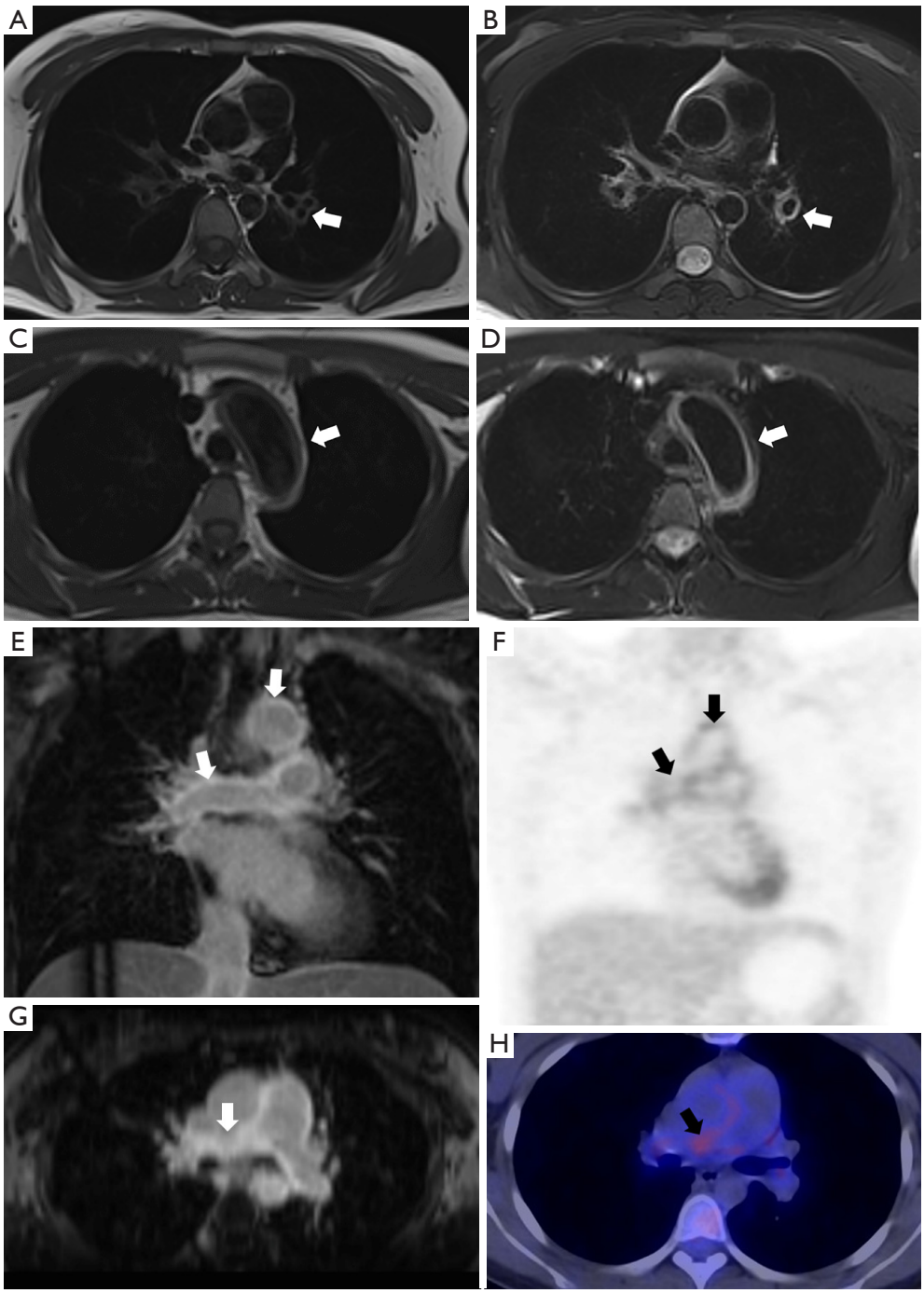

Figure 4 A 23-year-old female patient with no treatment of arteritis, who was in a clinically active phase. MRI shows arterial wall thickening in T1WI (A,C) and edema in T2WI (B,D) in the PA and aortic arch (white arrows). DE-MRI (E,G) shows arterial wall-delayed enhancement in the main PA, and the thoracic aorta and its branches (white arrows) in a coronal and axial view. FDG PET/CT images (F,H) show intense uptake by the aortic arch and the main PA and its branches (SUV_{max} 4.0, 2.9, 3.2, liver SUV_{max} 2.3) (black arrows) in the same view. MRI, magnetic resonance imaging; T1/T2WI, T1/T2 weighted imaging; PA, pulmonary artery; DE, delayed contrast-enhanced; FDG PET/CT, fluorodeoxyglucose positron emission tomography/computed tomography; SUV_{max}, maximum standardized uptake value.

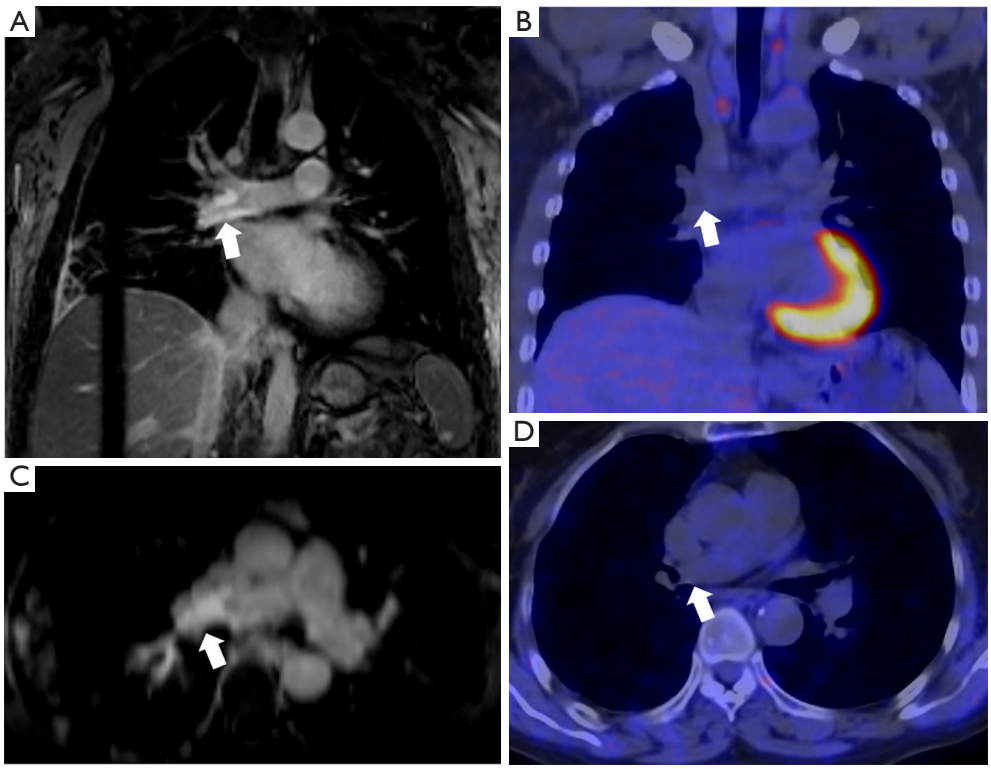

Figure 5 A 24-year-old female patient who received steroid and cyclophosphamide therapy for 4 months with active arteritis, who was in a clinically active phase. DE-MRI (A,C) shows delayed enhancement of wall in the right PA and the lower lobar artery (white arrows) in a coronal and oblique view (which is parallel to the long axis of the right PA). FDG PET/CT images (B,D) show no uptake by the right PA and lower lobar artery (SUV_{max} 1.6, 2.0, liver SUV_{max} 2.4) (white arrows) in the coronal and axial view. The black band of DE-MRI is the detection plane of breath navigation. DE-MRI, delayed contrast-enhanced magnetic resonance imaging; PA, pulmonary artery; FDG PET/CT, fuorodeoxyglucose positron emission tomography/computed tomography; SUV_{max}, maximum standardized uptake value.

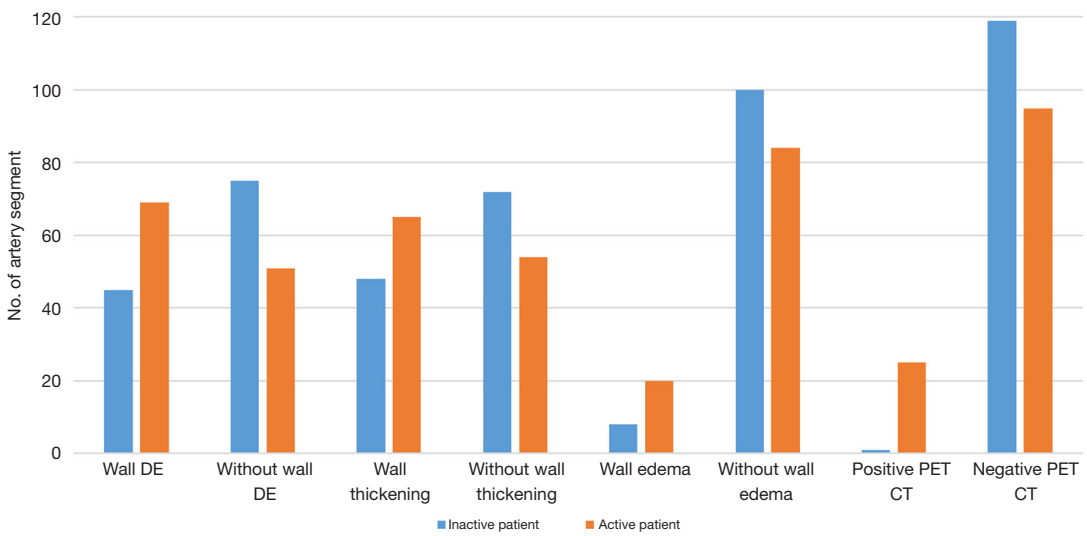

Figure 6 Association between image features and TAK activity in PA based on NIH criteria. DE, delayed contrast-enhancement; PET/CT, positron emission tomography/computed tomography; TAK, Takayasu's arteritis; PA, pulmonary artery; NIH, National Institutes of Health.

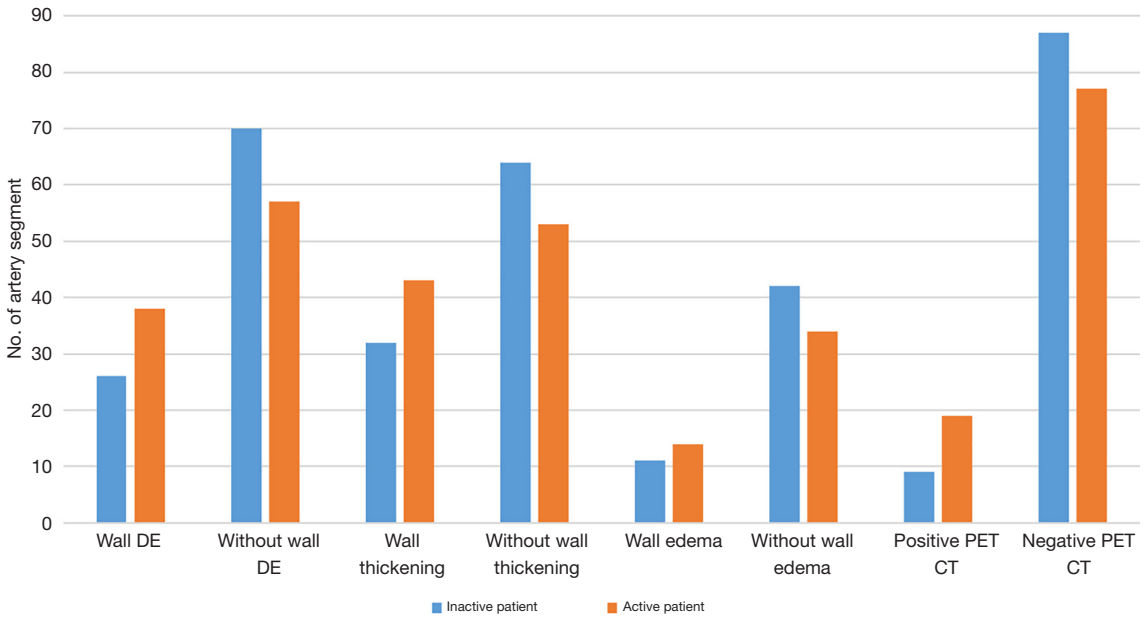

Figure 7 Association between image features and TAK activity in thoracic aorta based on NIH criteria. DE, delayed contrast-enhancement; PET/CT, positron emission tomography/computed tomography; TAK, Takayasu's arteritis; NIH, National Institutes of Health.

Table 3 Per-segment comparison between arterial wall DE and other MRI features of the PA

PA	Thickening+	Thickening–	Without edema	Edema	Abnormal lumen	Normal lumen
DE-MRI–	107	18	117	1	51	70
DE-MRI+	19	95	67	27	42	71

DE & thickening: Cohen's kappa =0.69 (P<0.001), percent agreement: 84.52%. DE & edema: Cohen's kappa =0.30 (P<0.001), percent agreement: 67.92%. DE & lumen: Cohen's kappa =0.05 (P=0.437), percent agreement: 52.13%. DE, delayed contrast-enhancement; MRI, magnetic resonance imaging; PA, pulmonary artery; DE-MRI+/–, positive/negative delayed enhancement category in comparison to the myocardium signal.

Table 4 Per-segment comparison between arterial wall DE and other MRI features of thoracic aorta

Thoracic aorta	Thickening+	Thickening–	Without edema	Edema	Abnormal lumen	Normal lumen
DE-MRI–	109	18	61	5	3	124
DE-MRI+	8	56	15	19	0	64

DE & thickening: Cohen's kappa =0.71 (P<0.001), percent agreement: 86.38%. DE & edema: Cohen's kappa =0.52 (P<0.001), percent agreement: 80.00%. DE & lumen: Cohen's kappa =0.016 (P=0.215), percent agreement: 35.07%. DE, delayed contrast-enhancement; MRI, magnetic resonance imaging; DE-MRI+/–, positive/negative delayed enhancement category in comparison to the myocardium signal.

with ESR, it showed significant diagnostic efficiency (AUC: 0.858, sensitivity: 0.833, specificity: 0.75, P=0.003, 95% CI: 0.71–1.00), followed by the wall DE combined with thickness (AUC: 0.736, sensitivity: 1.00, specificity: 0.417, P=0.05, 95% CI: 0.53–0.95), and finally the wall DE combined with edema (AUC: 0.73, P=0.057, 95% CI: 0.52–0.94). Although the latter 2 combined indicators showed a higher AUC, they lacked statistical significance.

Discussion

TAK is characterized by multiple patchy or segmental wall

Table 5 Comparisons of MRI features between PA and thoracic aorta in patients with active and inactive TAK

Variable	Patents with active TAK (n=12)				Patients without active TAK (n=12)			
	Thoracic aorta	PA	χ^2	P value	Thoracic aorta	PA	χ^2	P value
Wall DE, n (%)	38 (39.58%)	69 (57.50%)	6.85	0.009	26 (27.08%)	45 (37.50%)	2.62	0.105
Wall edema, n (%)	14 (29.17%)	20 (19.23%)	1.86	0.172	11 (20.75%)	8 (7.41%)	6.08	0.004
Wall thickening, n (%)	43 (44.79%)	66 (55%)	2.22	0.136	32 (33.68%)	48 (40%)	0.91	0.341
Abnormal lumen, n (%)	0	44 (38.59%)	46.44	<0.001	3 (3.13%)	49 (40.83%)	42.23	<0.001

MRI, magnetic resonance imaging; PA, pulmonary artery; TAK, Takayasu's arteritis; DE, delayed contrast-enhancement.

Table 6 Diagnostic performance of DE-MRI and PET/CT for the detection of TAK activity

Imaging method (n=24)	Sensitivity (%)	Specificity (%)	PPV (%)	NPV (%)	AUC (95% CI)	P value
Wall DE	91.7	66.7	73.3	88.9	0.729 (0.54–0.95)	0.047
PET/CT	75.0	91.7	90.0	78.6	0.833 (0.66–1.00)	0.006

DE-MRI, delayed contrast-enhanced magnetic resonance imaging; PET/CT, positron emission tomography/computed tomography; TAK, Takayasu's arteritis; PPV, positive predictive value; NPV, negative predictive value; AUC, area under the curve; CI, confidence interval.

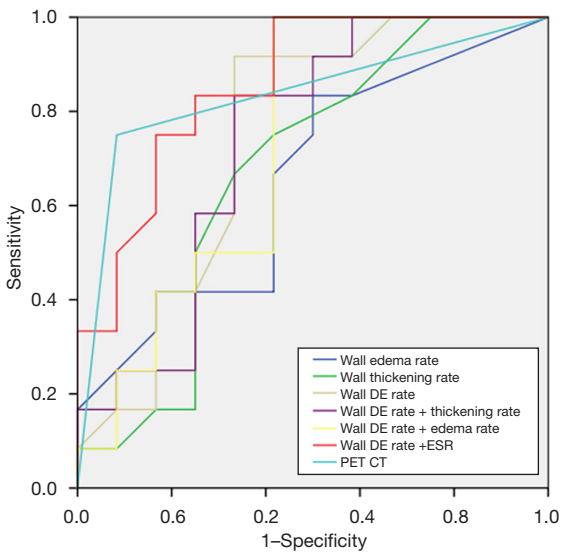

Figure 8 ROC analysis of image features for assessing TAK activity. The rate, arterial segments of positive MRI features divided by 18 segments; +, combined indicator. DE, delayed contrast-enhancement; ESR, erythrocyte sedimentation rate; PET/CT, positron emission tomography/computed tomography; ROC, receiver operating curve; TAK, Takayasu's arteritis; MRI, magnetic resonance imaging.

lesions, and segmental analysis can more accurately reflect the status of the disease. Most imaging studies on TAK activity have been based on per-patient analysis and have rarely reported PA lesions specifically. In this study, per-segment analysis was used, and it yielded valuable results. Firstly, active PA lesions in TAK can be detected using DE-MRI with a relatively high degree of agreement with PET/CT findings. Secondly, the consistency of wall DE and other imaging features (wall thickening, edema, and PET/CT findings) was higher in the thoracic aorta artery than that in the PA, and the incidence of wall DE in the PA was higher than that in the thoracic aorta in patients with active TAK according to NIH criteria. Thirdly, the wall DE showed better performance than wall thickness and edema for discriminating TAK activity. Moreover, DE-MRI combined with ESR enhanced the diagnostic efficacy of assessing TAK activity.

The histologic patterns of TAK are varied and can manifest as acute exudative inflammation, chronic and nonspecific productive inflammation, and granulomatous inflammation (26). These various histologic patterns may show as different features on imaging tools. PET/CT can detect abnormal metabolic activity in ongoing vascular inflammation and can be valuable in assessing vascular activity in patients with LVV (6).

Our previous study demonstrated that PET/CT can effectively evaluate PA activity in patients with TAK, and more than half of PET/CT active PA segments (54.9%) showed mural thickening (21). In this study we further found that PET/CT and wall DE had a high agreement in that 76.92% (20/26) of PET/CT active PA segments showed wall

DE. As a result, we suggested that wall DE on MRI might be related to PA activity. The wall DE representing chronic active vasculitis and granuloma formation was not definitely affected by short-term immunosuppression treatment. However, FDG uptake in PET/CT is very sensitive to immunosuppressive treatment (27). In the current study, 45.8% of patients received different types of steroids and/or other immunosuppressive therapies, which might have led to lower sensitivity of PCT/CT compared with DE-MRI. The low kappa value between the 2 imaging tools for both PA and thoracic aorta may therefore have been affected by drug therapy.

Wall edema and thickness of MRI are considered signs of acute inflammation of the vessel wall in LVV (6,28). The arterial wall DE may be associated with increased permeability (acute inflammation) and enlargement of the extracellular space of the arterial wall (nonspecific inflammation or fibrosis) (29). Previous studies have suggested that wall DE on MRI is a useful technique to identify inflammation and/or fibrosis of the thoracic aorta in patients with active TAK (8), and hence, wall DE is considered a characteristic of active TAK. PAI is a special type of TAK, which is rarely evaluated separately by imaging methods. This study found that wall DE on MRI was strongly associated with edema and thickening in both the thoracic aorta and the PA. In addition, the DE consistency in the thoracic aorta was higher than that in the PA. We speculate that there may be 2 reasons: one reason might be that the PA is easily affected by imaging resolution, as the PA has a thinner wall and more branches than the thoracic aorta; the second may be that the incidences of wall thickness and edema are lower than those of lumen stenosis, which is supported by the fact that TAK with PAI is often misdiagnosed as chronic pulmonary embolism.

Morphological abnormality of arterial lumen is a characteristic of TAK and of little value in indicating TAK activity (6). Consistent with previous research, our studies also showed that it was not associated with uptake of PET/CT (21) and wall DE on MRI. However, an increasing number of lumen locations was the strongest risk factor for an increased likelihood of pulmonary hypertension in patients with PAI (3).

Misdiagnosis of TAK is common and delays timely treatment. This study's results of a lesion-by-lesion analysis support DE-MRI as a highly sensitive, noninvasive method for determining TAK activity. Moreover, positive DE segments significantly differed between the PA and thoracic aorta in patients with clinically active TAK, and wall edema and thickness did not show any difference. This suggests that the wall DE is more sensitive in detecting active lesions in the PA than that in the thoracic aorta. The following reasons might partly explain the different findings between the thoracic aorta and PA: the particularity of the enrolled patients in this study might affect the incidence of wall DE, and PA was frequently involved with chronic inflammation in TAK patients with PAI. Further studies are needed to examine this issue.

Previous studies have also shown that persistent activity in imaging can be substantiated by biopsy data, which showed active, ongoing vasculitis. DE also has the potential of being an imaging marker for assessing arterial wall inflammation and response to therapy (30). Although it is probably not as specific a marker of inflammation as in the other areas of the body, such as myocardial diseases, the results of a patient-by-patient analysis using ROC analysis also substantiated a high diagnostic performance for assessing TAK activity, when compared with other MRI features. Admittedly, DE-MRI has a limited ability to exclude remodeling lesions of PA due to the imaging mechanism, but it can strengthen imaging evidence of disease activity in symptomatic patients with TAK.

Both the current study and previous research have indicated that serological indicators were not associated with PET/CT disease activity (31) or wall DE using MRI in patients with TAK. However, the diagnostic accuracy of wall DE combined with ESR was markedly improved, and became almost equivalent to that of PET/CT findings. This combined indicator highlights the superiority of the 2 methods. It could both reduce the false-positive effect of wall DE associated with wall fibrosis and increase the specificity of ESR.

In addition to the small sample size related to the underlying rarity of TAK, the current study has several other limitations, and technical issues also need to be considered. The cases included in this study were limited to patients with TAK and PAI, as all patients were recruited through a respiratory department. The arterial wall DE of MRI was performed by visual inspection of the images, and the time course of gadolinium enhancement remains to be optimized. The scanning field only included the thorax, which is not adequate for systemic artery disease. Moreover, the positive rate for ROC analysis was calculated using 18 segments, of which the inferior segmental arteries of PA were excluded due to imaging tool resolution limitations. The lack of a 'gold standard' is an inherent flaw of imaging methods to assess disease activity in TAK. There is

currently limited evidence-based data on DE-MRI analysis of PA lesions. Further studies are warranted to determine the efficiency of DE-MRI in patients with TAK and PAI.

Conclusions

In this study, DE-MRI exhibited appreciable agreement with PET/CT findings in detecting PA inflammation and identified active lesions both in the thoracic aorta and the PA. However, arterial wall DE was more valuable in the thoracic aorta than in the PA. Wall DE is better for the determination of TAK status than wall thickening and edema on MRI, and slightly worse than PET/CT findings. The combination of wall DE and ESR improves the efficiency of assessing TAK activity. Therefore, DE-MRI may be a valuable addition to PET/CT for identifying patients with active PAI and has important potential application value in that MRI is widely available, cheaper, and emits no radiation. In some clinical situations where PET/CT is not available, DE-MRI can be used as a surrogate for PET scan activity.

Acknowledgments

Funding: This work was supported by Beijing Hospitals Authority Clinical Medicine Development of Special Funding Support (No. ZYLX202105) and the National Natural Science Foundation of China (Nos. 81871380 and 81871328).

Footnote

Reporting Checklist: The authors completed the STARD reporting checklist. Available at https://qims.amegroups.com/article/view/10.21037/qims-22-130/rc

Conflicts of Interest: All authors completed the ICMJE uniform disclosure form (available at https://qims.amegroups.com/article/view/10.21037/qims-22-130/coif). The authors have no conflicts of interest to declare.

Ethical Statement: The authors are accountable for all aspects of the work in ensuring that questions related to the accuracy or integrity of any part of the work are appropriately investigated and resolved. The patients of this imaging subgroup analysis participated in a prospective study on TAK, which was approved by the Ethics Committee of Beijing Chaoyang Hospital (No. 2017-K-127), and all participants were aware of, and agreed to participate in, this study. The study was conducted in accordance with the Declaration of Helsinki (as revised in 2013). Informed consent was provided by all individual participants included in the study.

References

1. Kerr GS, Hallahan CW, Giordano J, Leavitt RY, Fauci AS, Rottem M, Hoffman GS. Takayasu arteritis. Ann Intern Med 1994;120:919-29.
2. Bicakcigil M, Aksu K, Kamali S, Ozbalkan Z, Ates A, Karadag O, et al. Takayasu's arteritis in Turkey - clinical and angiographic features of 248 patients. Clin Exp Rheumatol 2009;27:S59-64.
3. Gong J, Yang Y, Ma Z, Guo X, Wang J, Kuang T, Yang S, Li J, Miao R, Huang K. Clinical and imaging manifestations of Takayasu's arteritis with pulmonary hypertension: A retrospective cohort study in China. Int J Cardiol 2019;276:224-9.
4. Yang L, Zhang H, Jiang X, Zou Y, Qin F, Song L, Guan T, Wu H, Xu L, Liu Y, Zhou X, Bian J, Hui R, Zheng D. Clinical manifestations and longterm outcome for patients with Takayasu arteritis in China. J Rheumatol 2014;41:2439-46.
5. Barra L, Kanji T, Malette J, Pagnoux C; CanVasc. Imaging modalities for the diagnosis and disease activity assessment of Takayasu's arteritis: A systematic review and meta-analysis. Autoimmun Rev 2018;17:175-87.
6. Quinn KA, Ahlman MA, Malayeri AA, Marko J, Civelek AC, Rosenblum JS, Bagheri AA, Merkel PA, Novakovich E, Grayson PC. Comparison of magnetic resonance angiography and 18F-fluorodeoxyglucose positron emission tomography in large-vessel vasculitis. Ann Rheum Dis 2018;77:1165-71.
7. Desai MY, Stone JH, Foo TK, Hellmann DB, Lima JA, Bluemke DA. Delayed contrast-enhanced MRI of the aortic wall in Takayasu's arteritis: initial experience. AJR

Am J Roentgenol 2005;184:1427-31.
8. Spira D, Xenitidis T, Henes J, Horger M. MRI parametric monitoring of biological therapies in primary large vessel vasculitides: a pilot study. Br J Radiol 2016;89:20150892.
9. Maurus S, Sommer NN, Kooijman H, Coppenrath E, Witt M, Schulze-Koops H, Czihal M, Hoffmann U, Saam T, Treitl KM. 3D black-blood 3T-MRI for the diagnosis of abdominal large vessel vasculitis. Eur Radiol 2020;30:1041-4.
10. Liu M, Liu W, Li H, Shu X, Tao X, Zhai Z. Evaluation of takayasu arteritis with delayed contrast-enhanced MR imaging by a free-breathing 3D IR turbo FLASH. Medicine (Baltimore) 2017;96:e9284.
11. Andrews J, Al-Nahhas A, Pennell DJ, Hossain MS, Davies KA, Haskard DO, Mason JC. Non-invasive imaging in the diagnosis and management of Takayasu's arteritis. Ann Rheum Dis 2004;63:995-1000.
12. Zhang X, Zhou J, Sun Y, Shi H, Ji Z, Jiang L. 18F-FDG-PET/CT: an accurate method to assess the activity of Takayasu's arteritis. Clin Rheumatol 2018;37:1927-35.
13. Lee SW, Kim SJ, Seo Y, Jeong SY, Ahn BC, Lee J. F-18 FDG PET for assessment of disease activity of large vessel vasculitis: A systematic review and meta-analysis. J Nucl Cardiol 2019;26:59-67.
14. Slart RHJA; EANM Committee Coordinator. FDG-PET/CT(A) imaging in large vessel vasculitis and polymyalgia rheumatica: joint procedural recommendation of the EANM, SNMMI, and the PET Interest Group (PIG), and endorsed by the ASNC. Eur J Nucl Med Mol Imaging 2018;45:1250-69.
15. Dejaco C, Ramiro S, Duftner C, Besson FL, Bley TA, Blockmans D, Brouwer E, Cimmino MA, Clark E, Dasgupta B, Diamantopoulos AP, Direskeneli H, Iagnocco A, Klink T, Neill L, Ponte C, Salvarani C, Slart RHJA, Whitlock M, Schmidt WA. EULAR recommendations for the use of imaging in large vessel vasculitis in clinical practice. Ann Rheum Dis 2018;77:636-43.
16. van der Geest KSM, Treglia G, Glaudemans AWJM, Brouwer E, Sandovici M, Jamar F, Gheysens O, Slart RHJA. Diagnostic value of 18FFDG-PET/CT for treatment monitoring in large vessel vasculitis: a systematic review and meta-analysis. Eur J Nucl Med Mol Imaging 2021;48:3886-902.
17. Grayson PC, Alehashemi S, Bagheri AA, Civelek AC, Cupps TR, Kaplan MJ, Malayeri AA, Merkel PA, Novakovich E, Bluemke DA, Ahlman MA. 18 F-Fluorodeoxyglucose-Positron Emission Tomography As an Imaging Biomarker in a Prospective, Longitudinal Cohort of Patients With Large Vessel Vasculitis. Arthritis Rheumatol 2018;70:439-49.
18. Dashora HR, Rosenblum JS, Quinn KA, Alessi H, Novakovich E, Saboury B, Ahlman MA, Grayson PC. Comparing Semiquantitative and Qualitative Methods of Vascular 18F-FDG PET Activity Measurement in Large-Vessel Vasculitis. J Nucl Med 2022;63:280-6.
19. Tateishi U, Tsuchiya J, Yokoyama K. Large vessel vasculitis: imaging standards of 18F-FDG PET/CT. Jpn J Radiol 2021;39:225-32.
20. Choe YH, Han BK, Koh EM, Kim DK, Do YS, Lee WR. Takayasu's arteritis: assessment of disease activity with contrast-enhanced MR imaging. AJR Am J Roentgenol 2000;175:505-11.
21. Gao W, Gong JN, Guo XJ, Wu JY, Xi XY, Ma ZH, Yang YH, Yang MF. Value of 18F-fluorodeoxyglucose positron emission tomography/computed tomography in the evaluation of pulmonary artery activity in patients with Takayasu's arteritis. Eur Heart J Cardiovasc Imaging 2021;22:541-50.
22. Sharma BK, Jain S, Suri S, Numano F. Diagnostic criteria for Takayasu arteritis. Int J Cardiol 1996;54 Suppl:S141-7.
23. Jiang L, Li D, Yan F, Dai X, Li Y, Ma L. Evaluation of Takayasu arteritis activity by delayed contrast-enhanced magnetic resonance imaging. Int J Cardiol 2012;155:262-7.
24. Martínez-Rodríguez I, Martínez-Amador N, Banzo I, Quirce R, Jiménez-Bonilla J, De Arcocha-Torres M, Ibáñez-Bravo S, Lavado-Pérez C, Bravo-Ferrer Z, Blanco R, González-Gay MA, Carril JM. Assessment of aortitis by semiquantitative analysis of 180-min 18F-FDG PET/CT acquisition images. Eur J Nucl Med Mol Imaging 2014;41:2319-24.
25. Bucerius J, Hyafil F, Verberne HJ, Slart RH, Lindner O, Sciagra R, Agostini D, Übleis C, Gimelli A, Hacker M; Cardiovascular Committee of the European Association of Nuclear Medicine (EANM). Position paper of the Cardiovascular Committee of the European Association of Nuclear Medicine (EANM) on PET imaging of atherosclerosis. Eur J Nucl Med Mol Imaging 2016;43:780-92.
26. Vaideeswar P, Deshpande JR. Pathology of Takayasu arteritis: A brief review. Ann Pediatr Cardiol 2013;6:52-8.
27. Nielsen BD, Gormsen LC, Hansen IT, Keller KK, Therkildsen P, Hauge EM. Three days of high-dose glucocorticoid treatment attenuates large-vessel 18F-FDG uptake in large-vessel giant cell arteritis but with a limited impact on diagnostic accuracy. Eur J Nucl Med Mol

Imaging 2018;45:1119-28.
28. Bley TA, Markl M, Schelp M, Uhl M, Frydrychowicz A, Vaith P, Peter HH, Langer M, Warnatz K. Mural inflammatory hyperenhancement in MRI of giant cell (temporal) arteritis resolves under corticosteroid treatment. Rheumatology (Oxford) 2008;47:65-7.
29. Kato Y, Terashima M, Ohigashi H, Tezuka D, Ashikaga T, Hirao K, Isobe M. Vessel Wall Inflammation of Takayasu Arteritis Detected by Contrast-Enhanced Magnetic Resonance Imaging: Association with Disease Distribution and Activity. PLoS One 2015;10:e0145855.
30. Adler S, Sprecher M, Wermelinger F, Klink T, Bonel H, Villiger PM. Diagnostic value of contrast-enhanced magnetic resonance angiography in large-vessel vasculitis. Swiss Med Wkly 2017;147:w14397.
31. Arnaud L, Haroche J, Malek Z, Archambaud F, Gambotti L, Grimon G, Kas A, Costedoat-Chalumeau N, Cacoub P, Toledano D, Cluzel P, Piette JC, Amoura Z. Is (18) F-fluorodeoxyglucose positron emission tomography scanning a reliable way to assess disease activity in Takayasu arteritis? Arthritis Rheum 2009;60:1193-200.

Cite this article as: Guo X, Liu M, Liu M, Ma Z, Gong J, Yang Y, Gao W, Wu J, Yang Q, Yang MF. Delayed contrast-enhanced magnetic resonance imaging enables detection of pulmonary artery lesions in Takayasu's arteritis. Quant Imaging Med Surg 2023;13(1):145-159. doi: 10.21037/qims-22-130

